

Spectral Emittance Characteristics of Powdery and Molten Coal Ashes

Fabian Greffrath¹, Martin Schiemann¹, Viktor Scherer¹ and Alfred Gwosdz²

¹Department of Energy Plant Technology (LEAT), Ruhr University Bochum, Germany;

²Hitachi Power Europe GmbH, Duisburg, Germany

KEYWORDS: radiation, emittance, ash, powder, structure, composition, sintering, fusion

ABSTRACT

Spectral emittances of two lignite and two bituminous coal ashes have been measured in the spectral range between 980 nm and 17020 nm at temperatures from about 500°C to 1100°C in order to investigate experimentally the effect of heat treatment. From each type of ash two samples have been prepared, one from untreated laboratory ash and one from heat-treated ash which has been heated up to a temperature of 1400°C for one hour. The emittance measurements of these eight specimens show that heat treatment may have manifold effects on both the physical structure and the mineralogical composition of ashes and thus on their emittance characteristics. The underlying mechanisms of these modifications and their impact on the heat transfer in an industrial boiler will be discussed.

INTRODUCTION

Radiation is the dominating heat transfer mechanism in solid fuel fired industrial furnaces. Thus, for a reliable heat balance of a plant, the knowledge of the optical properties of all media participating in radiation exchange is required. This includes the heat exchanger surfaces which are usually covered with a layer of ashes and slags. However, the optical properties of sintered or even fused ashes may differ significantly from those of laboratory ashes prepared and analyzed under normative conditions (i.e. at 815°C). Due to thermal treatment, both the physical structure of the surface as well as the chemical and mineralogical composition of an ash may undergo substantial changes that directly influence its heat absorption characteristics.^{2, 5, 8}

According to electromagnetic wave theory, radiation incident on an optically smooth surface gets partly reflected and partly propagates through the material. The decisive optical material property in this process is the complex refractive index $m = n - ik$. Here, the real refractive index n is the phase speed within the material relative to vacuum and determines the reflected and transmitted fractions of radiation. The absorption index k indicates the amount of absorption loss during the propagation through the medium. Both indices are determined by the microscopic inner structure of the material and thus its chemical and mineralogical composition. They typically vary with wavelength and

temperature and are hardly accessible by experimental means for inhomogeneous media such as ashes and slags.³

However, slag surfaces are made up of agglomerated particles and are thus generally not optically smooth. Consequently, a significant amount of radiation will be scattered at the surface which will be measured as an effective reflectance. The decisive property for radiation scattering is the size parameter $\chi = \pi d / \lambda$, where d is the characteristic diameter of a scattering center and λ is the radiation wavelength. The amount of scattering increases as χ approaches towards unity and may even exceed the influence of the aforementioned optical indices with regard to radiation interaction.^{2, 5, 7} The global material properties – emittance, absorbance, transmittance and reflectance – result from the interrelation of the aforementioned optical indices and size parameters.

In order to investigate the effect of heat treatment on the physical and mineralogical structure of ashes and to show the resulting differences in the optical properties, temperature dependent spectral emittances of four different coal ashes have been measured in the wavelength range between 980 nm and 17020 nm at temperatures from about 500°C to 1100°C. From each type of ash two samples have been prepared, one from untreated laboratory ash and one from heat-treated ash which has been heated up to a temperature of 1400°C for one hour. The experimental results are subject of the current paper.

EXPERIMENTAL SETUP AND PROCEDURE

All experiments described in this paper have been carried out using the radiation test rig of the department of energy plant technology (LEAT) at the Ruhr-University Bochum, Germany.⁸ This test rig, as depicted in Fig. 1, consists of two main parts: The first part comprises the heating unit which holds both the sample in the sample holder and the reference cavity radiator (“blackbody”), whereas the second part consists of the spectral radiometer.

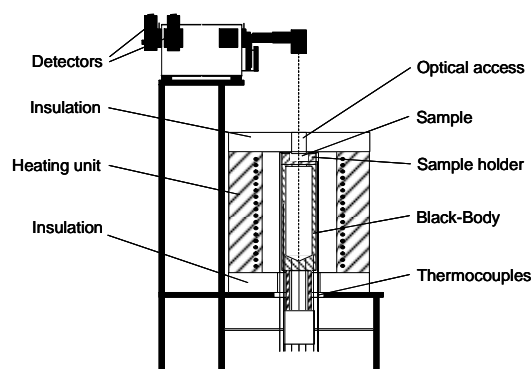


Fig. 1: Radiation test rig

The heating element is a vertical, hollow cylindrical electric furnace which is used to heat both the sample and the reference radiator up to the measuring temperatures. To avoid heat loss it is covered with insulating slabs at the top and bottom faces. The reference radiator is made of a heat resistant nickel-based alloy and laid out as a

cylindrical cavity radiator with an inner diameter of 50 mm and a conical bottom with a central cavity length of 135 mm.

The cylindrical samples have a diameter of 22,5 mm and 4 mm height and sit in a sample holder. The sample holder lies on top of the reference radiator, which sits on a ceramic tube that can be shifted up and down inside the heating element. For measurement of the sample radiation the sample holder is shifted up to the top of the heating element directly underneath the insulation slab. The radiation emitted vertically by the sample surface leaves the heating element through the optical access and is detected by the spectral radiometer. Temperatures are determined by type K thermocouples in the sample and the sample holder as well as type N thermocouples in the bottom of the reference radiator.

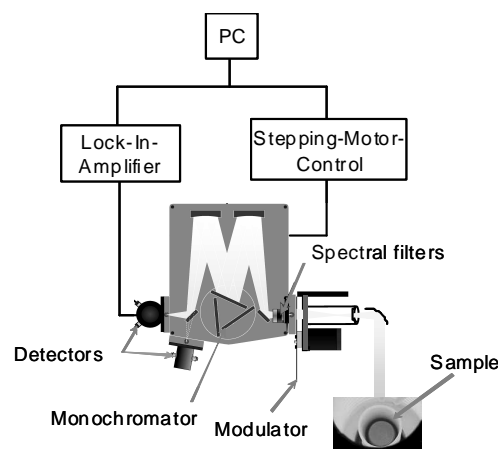


Fig. 2: Spectral Radiometer System

Radiation measurements are carried out by a computer-aided spectral radiometer system which is based on a Czerny-Turner grating monochromator, see Fig. 2 for a detailed view. The thermal radiation emitted by the sample (or the reference radiator respectively) passes through an optical access in the top insulation and hits a gold-plated off-axis mirror that reflects the radiation signal onto the entrance slit of a monochromator system. In front of this slit the signal is periodically intercepted by a rotating aperture plate, the chopper, which by this means imposes a modulation of known frequency and phase on the signal. This modulation is synchronized with a lock-in amplifier which in turn provides for a high signal-to-noise ratio. Inside the monochromator the radiation is collimated by a curved mirror and diffracted by one of three gratings. The gratings – each with a different grating constant – are mounted on a rotatable platform. The dispersed radiation is then reflected by another mirror and refocused on the exit slit, where a liquid N₂-cooled MCT-detector (Mercury-Cadmium-Tellur) is installed. To avoid superimposition of diverse diffraction maxima of different wavelengths, a filter wheel with six edge filters is inserted into the optical path. Stepping motors that select the appropriate optical filter as well as the grating and diffraction angle according to the target wavelength are controlled by computer software. A laser pointer is used prior to the measurements for the precise alignment of the spectrometer with the sample.

Data acquisition

The determination of the spectral emittances is based on a static radiation comparison method, in which the ratios of the detected radiance signals from the sample $S_S(\lambda, T)$ and the aforementioned reference radiator at the same temperature and wavelength $S_R(\lambda, T)$ are calculated:

$$\varepsilon(\lambda, T) = \frac{S_S(\lambda, T)}{S_R(\lambda, T)} \quad (1)$$

The spectral emittances are determined in the wavelength range from 980 nm to 17020 nm using a step size of 40 nm, resulting in a total of 402 records per measurements. The measuring temperatures can be adjusted in a range between about 500°C and 1100°C by means of a thyristor-operated furnace control. The lower temperature limitation results from the operational range of the heating element, whereas the upper limit is restricted by the thermal stress of the reference radiator material. The wavelength interval is limited by the sensitivity of the detector. The step size of 40 nm has been chosen as a good compromise between spectral resolution and acceptable measurement time.

In this paper the experimental results for each sample are presented as average emittances that are calculated by weighting the spectral emittances $\varepsilon(\lambda, T)$ with the radiation intensity $p(\lambda, T)$ of a cavity radiator as described by PLANCK'S law at the corresponding temperature and wavelength:

$$\bar{\varepsilon}(T) = \frac{\int_{\lambda_1}^{\lambda_2} \varepsilon(\lambda, T) \cdot p(\lambda, T) d\lambda}{\int_{\lambda_1}^{\lambda_2} p(\lambda, T) d\lambda} \quad (2)$$

Sample preparation

The powdery samples are prepared by mechanical compression of the ash into the sample holder using a pressure of 200 bar with a punch of 22 mm diameter. To allow for the insertion of a 1 mm type K thermocouple, a radial drill hole with 1,1 mm diameter is applied using a conventional drilling tool when the sample is still in the press. This allows for a placement of the thermocouple tip 2 mm underneath the centre of the sample surface.

The molten and sintered ash samples have been prepared similarly by drilling a cylinder of 22 mm diameter out of the solid material with a hollow drill, cutting a slice of 4 mm thickness off the surface and application of a radial drill hole for the thermocouple.

RESULTS

Heat-treated ash samples have been prepared from two lignite ashes, Hambach and Schleenhain, as well as two bituminous ashes, Prosper and Blair Athol, for comparison with the corresponding powdery ashes produced under normative conditions. To produce the molten specimen, small portions of the perspective ashes have been heated up in ceramic cylinders and held at a temperature of 1400°C for one hour.

Elementary analysis results for the four untreated laboratory ashes can be found in Tab. 1 below. Photographs of the four molten and sintered ashes in the ceramic cylinders after the heat treatment can be found in Fig. 3.

Tab. 1: Elementary Analyses of the untreated laboratory ashes

| | Hambach | Prosper | Blair Athol |
|------------------------------------|---------|---------|-------------|
| SiO₂ | 5,3 | 50,3 | 60,5 |
| Al₂O₃ | 1,9 | 27,3 | 35,1 |
| TiO₂ | 0,3 | 1,2 | 1,9 |
| Fe₂O₃ | 11,1 | 8,9 | 1,4 |
| CaO | 37,5 | 2,7 | 0,3 |
| MgO | 17,5 | 1,9 | 0,2 |
| Na₂O | 6,4 | 1,5 | 0,2 |
| K₂O | 0,6 | 3,5 | 0,4 |
| SO₃ | 18,6 | 2,6 | 0,5 |
| P₂O₅ | 0,1 | 0,8 | 0,3 |



Fig. 3: Molten ash samples: Hambach (TL), Prosper (TR), Blair Athol (BL) and Schleenhain (BR)

Hambach

The photograph of the heat-treated Hambach sample in the ceramic cylinder in Fig. 3 shows that the initial ash layer – which was about 3 cm thick – has sintered and shrunk to form a truncated cone of green-gray color and about 1,5 cm height surrounded by a thin light-green ring of matter that must have been completely fused during the heat treatment.

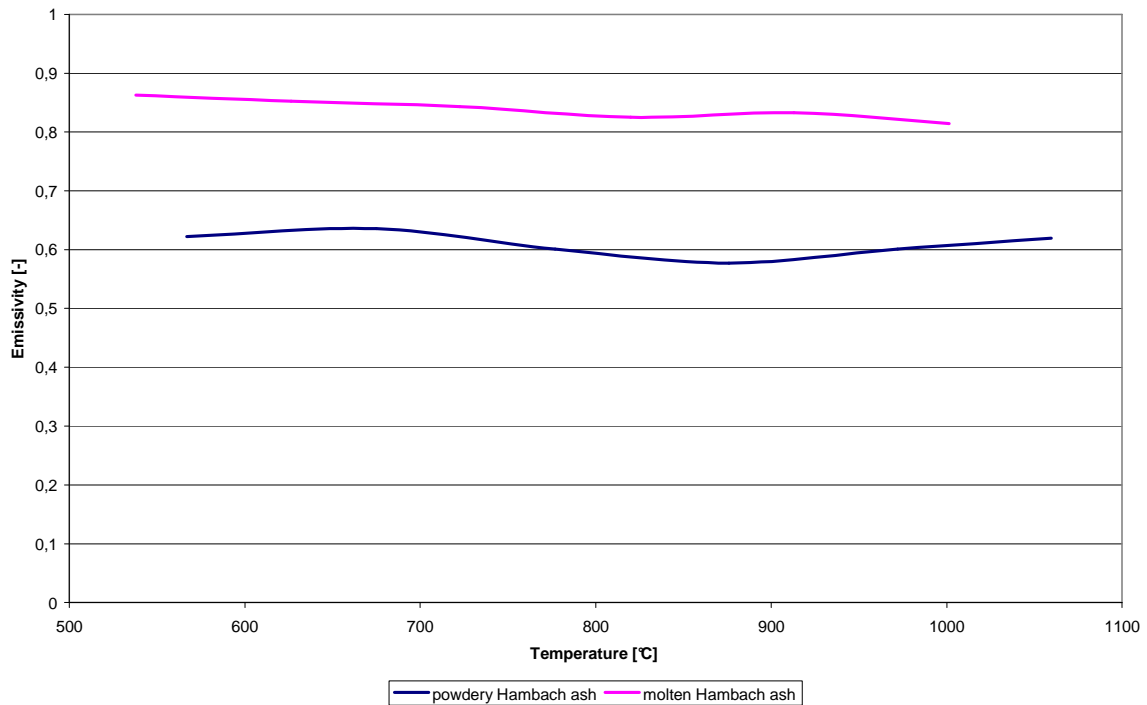


Fig. 4: Average emittances of powdery and molten Hambach ash

The average emittances of both the untreated and the heat-treated Hambach samples are shown in Fig. 4. The molten sample features very high emittances on levels at least 0,2 above the powdery ash over the whole examined temperature range. Apparently, the sintered matter has transformed into a glass-like volume radiator with a lower absorption index and thus higher transmittance than the powdery sample while still featuring low reflectance at the surface. This allows for transmission of radiation from inner layers of the specimen and thus leads to a high overall radiation emittance. The emittance increase of ashes at temperatures beyond the softening point and the hysteresis, i.e. the irreversibility of this process by subsequent cooling below this point, has already been observed by other authors.^{2, 4, 5}

Prosper

As shown in Fig. 3, the molten Prosper ash has completely collapsed and formed a silvery-gray crust at the bottom of the ceramic cylinder. The craters and enclosed blisters indicate that the matter has boiled during the heat-treatment. The surface of the sample is lustrous and highly reflective and thus shows typical characteristics of a metallic surface.

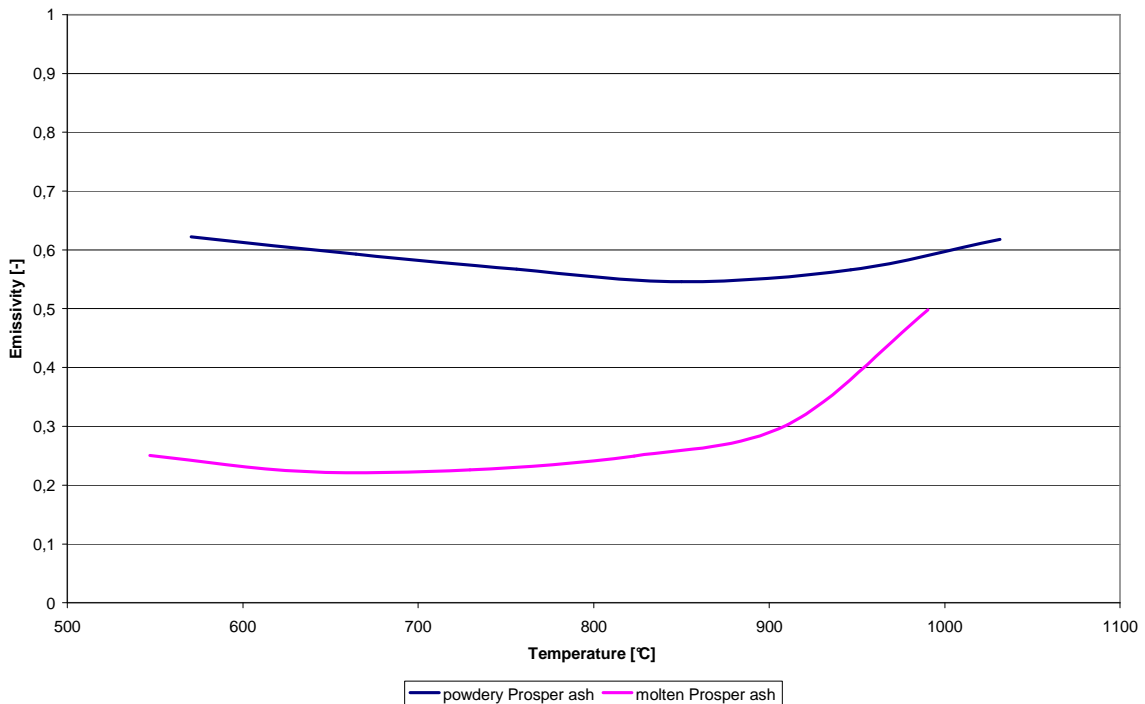


Fig. 5: Average emittances of powdery and molten Prosper ash

As shown in Fig. 5, the total emittance of the molten Prosper sample is generally low, it never exceeds over 0,5 across the whole examined temperature range. In comparison with the emittance curve of the untreated powdery ash it lies between 0,2 and 0,3 below, at least up to a temperature of about 900°C. From this temperature on, the emittances of both samples increase and would probably even meet at the same emittance value of about 0,65 at a temperature of about 1050°C. This point, though, has not been reached during this experiment.

The optical appearance of the molten Prosper sample is radically different from the other investigated samples as its lustrous and nearly specular reflective surface resembles the optical characteristics of metals surfaces. The reason for this may be a shift in the mineralogical composition of the material towards one that is dominated by metallic bond¹, e.g. pyrite. This in turn involves drastic changes in the optical properties. As a consequence, the matter becomes opaque for a wide wavelength range so both absorption and emission are suppressed as well as transmission of radiation from the sample volume. The emittance increase at higher measuring temperatures for both the

molten and the powdery ash samples could be attributed to a softening of the matter which again leads to a transmittance increase.

Blair Athol

As shown in Fig. 3, the heat-treated Blair Athol ash has formed a shrunken sintered block quite similar to the Hambach sample discussed above. In contrast to the Hambach sample, which had a more homogenous glass-like structure, the Blair Athol sample is more porous and features haptics and appearance similar to sandstone. Hence, its physical structure has not vastly changed from the untreated compressed powder form.

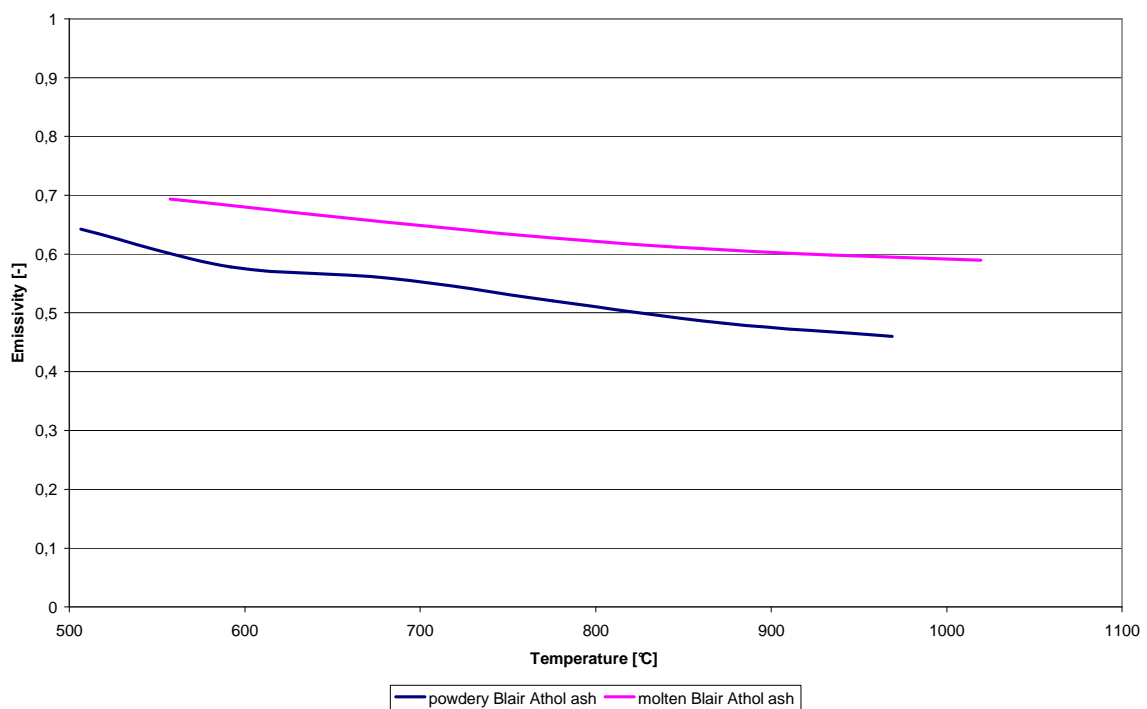


Fig. 6: Average emittances of powdery and molten Blair Athol ash

The total emittances of the powdery and the molten Blair Athol ash are shown in Fig. 6 and feature nearly parallel curves with the one of the heat-treated ash about 0,1 higher across the whole temperature range. It can be said that the similar physical structures of the compressed powdery ash and the molten ash are indeed reflected by their emittance characteristics.

In the case of the Blair Athol ash, the slightly higher emittance of the sintered sample should not be attributed to shifts in the values of the optical indices; the visible structure of the sample is still too similar to the initial ash powder to justify this assumption. Instead, the emittance increase is most probably caused by changes on the sample surface, namely the agglomeration of powder particles and the formation of bigger grains and cavities. By this means, the particle geometry consequently shifts out of the

order of magnitude of the wavelengths of the thermal radiation, which in turn makes the surface increasingly unsuitable for light scattering. So the focus of interaction between the surface and radiation shifts away from scattering and reflection more towards absorption and emission.^{6,7}

Schleenhain

As shown in Fig. 3, the Schleenhain ash was completely molten by the heat treatment and covered the bottom of the ceramic cylinder forming a smooth glass-like layer. Apparently, the material did not boil, since no craters or embedded blisters could be found in the matter. The surface is very plain, but not as smooth and lustrous as the one of the Prosper sample. Instead, small facets have formed on the surface that sparkle in the light and provide for a rather glassy and brittle appearance of the sample. Indeed, the material came out as highly fragile and it required some special treatment to get the sample disc separated and the drill hole applied.

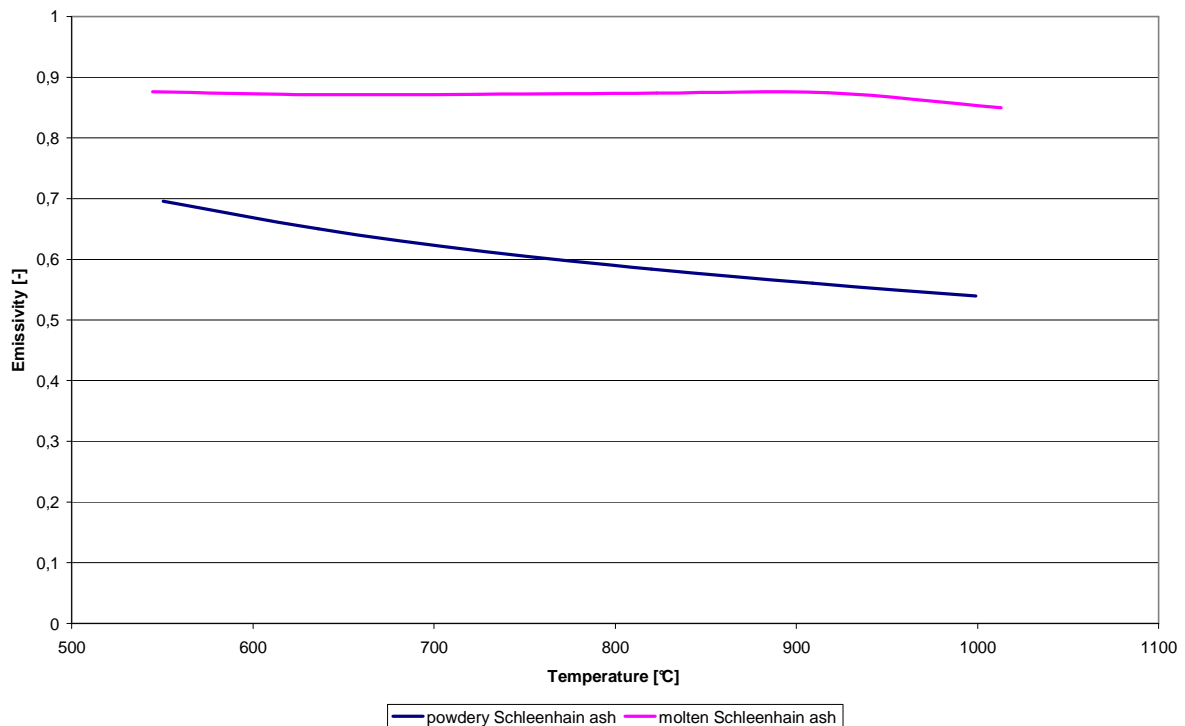


Fig. 7: Average emittances of powdery and molten Schleenhain ash

The emittances of the molten Schleenhain sample are on a nearly constant level above 0,8 and are therefore the highest values that have been measured in the course of this experimental series. Similar to the other molten lignite ash sample, Hambach, the temperature treatment has apparently vastly decreased the absorption index of the molten Schleenhain sample which involves increasing its transmittance. Hence, the matter took the characteristics of a glass-like volume radiator, so radiation from inner layers of the specimen may pass through the material and contribute to a high overall radiation emittance.

SUMMARY

To sum up the findings of the experimental series presented here it can be said that the heat-treatment and melting of an ash can have manifold effects on its emittance characteristics. In the cases of the lignites, Hambach and Schleenhain, the ash powders sintered or melted to form glass-like solid blocks with high transmittance and low reflectance characteristics which feature distinctly increased emittances. The bituminous Prosper ash also melted, but developed a smooth, lustrous and highly reflecting surface, which shares many characteristics with a metal surface and features in a drastic emittance decrease. This effect is attributed to a vast shift in the mineralogical composition that is dominated by metallic bonding. Finally, the Blair Athol ash sintered, but remained grainy and thus did neither radically change its mineralogical nor its emittance characteristics. Instead, due to the reduced ability to scatter light and the formation of bigger cavities on its surface, the emittance of this ash has only slightly increased.

According to KIRCHHOFF'S Law of the equality of emission and absorption of a surface in thermal equilibrium, the ash emittances measured and presented here are directly correlated to the ash absorbance characteristics. This means that at temperatures below 900°C the amount of heat absorbed by a heat exchanger surface by means of radiation may differ by a factor of up to nearly 4 depending on whether the surface is covered by a slag of molten Schleenhain or Prosper ash. According to Wall et al.⁵, reducing the wall emittance in a power station furnace from 0,8 to 0,4 will increase the furnace exit temperature by 110°C, corresponding to a decrease in furnace efficiency of 5,5%.

Since all ashes have undergone the same laboratory preparation and heat treatment, the differences in their emittance characteristics must be caused by their dissimilar initial mineralogical compositions. However, at the current state of the project, further research in this regard has still to be carried out.

ACKNOWLEDGEMENT

This research project has been facilitated by financial support of Hitachi Power Europe GmbH, which is gratefully acknowledged.

LITERATURE

- [1] PAULING, L.: The Nature of the Chemical Bond, 3rd Ed., Cornell University Press, 1960
- [2] BOOW, J.; GOARD, P. R. C.: Fireside deposits and their effect on heat transfer in a pulverized-fuel-fired boiler: Part III. The influence of the physical characteristics of the deposit on its radiant emittance and effective thermal conductance, J. Inst. Fuel 42, 1969, 412–419
- [3] GOODWIN, D. G.; MITCHNER, M.: Infrared Optical Constants of Coal Slags: Dependence on Chemical Composition, J. Thermophysics 3, 1989, 53–60

- [4] MARKHAM, J. R.; BEST, P. E.; SOLOMON, P. R.; YU, Z. Z.: Measurement of Radiative Properties of Ash and Slag by FT-IR Emission and Reflection Spectroscopy, *J. Heat Transfer* 114, 1992, 458–464
- [5] WALL, T. F.; BHATTACHARYA, S. P.; ZHANG, D. K.; GUPTA, R. P.; HE, X.: The properties and thermal effects of ash deposits in coal-fired furnaces, *Prog. Energy Combust. Sci.* 19, 1993, 487–504
- [6] RICHARDS, G. H.; HARB, J. N.; BAXTER, L. L.; BHATTACHARYA, S.; GUPTA, R. P.; WALL, T. F.: Radiative Heat Transfer in Pulverized-Coal-Fired Boilers – Development of the Absorptive/Reflective character of Initial Ash Deposits, Twenty-fifth Symposium (International) on Combustion, 1994, 511–518
- [7] ZYGARLICHE, C. J.; MCCOLLOR, D. P.; CROCKER, C. R.: Ash Emissivity Characterization and Prediction, Final Report, Energy & Environmental Research Center, North Dakota, 1999
- [8] BOHNES, S.; SCHERER, V.; LINKA, S.; NEUROTH, M.; BRÜGGEMANN, H.: Spectral Emissivity Measurements of Single Mineral Phases and Ash Deposits (HT2005-72099), ASME Summer Heat Transfer Conference, San Francisco, 2005